American Mineralogist, Volume 102, pages 1006–1020, 2017

Controls on trace-element partitioning among co-crystallizing minerals: Evidence from the Panzhihua layered intrusion, SW China

Lie-Meng Chen[1], Xie-Yan Song[1,*], Rui-Zhong Hu[1], Song-Yue Yu[1], Hai-Long He[1,2], Zhi-Hui Dai[1], Yu-Wei She[1,2], and Wei Xie[3]

[1]State Key Laboratory of Ore Deposit Geochemistry, Institute of Geochemistry, Chinese Academy of Sciences, Guiyang, 550081, P.R. China
[2]University of Chinese Academy of Sciences, Beijing, 100049, P.R. China
[3]State Key Laboratory of Isotope Geochemistry, Guangzhou Institute of Geochemistry, Chinese Academy of Sciences, Guangzhou, 510640, P.R. China

Abstract

The factors and processes that control trace-element partitioning among co-crystallizing cumulus minerals in layered intrusions have long been controversial. Here we address this issue using new laser ablation ICP-MS trace element data for magnetite, ilmenite, and clinopyroxene from the Panzhihua layered intrusion in the Emeishan large igneous province, SW China. The cumulus minerals display strong Ni, Co, and Cr depletions, indicative of parental magmas low in concentration of these elements probably due to prior sulfide removal and the fractionation of chromite or Cr-magnetite in a staging magma chamber at depth. Both magnetite and clinopyroxene show cyclical variations in some transition elements (e.g., Cr, V, and Ni) along the stratigraphic section. The average concentrations of these transition elements in magnetite are positively correlated with those in clinopyroxene, likely resulting from co-crystallization of magnetite and clinopyroxene. The incompatible element (e.g., Zr, Hf, and Nb) concentrations of the cumulus minerals from the Lower Zone are highly variable compared to those of the Middle and Upper Zones. These large variations in trace element compositions are attributed to a "trapped liquid shift" in the Lower Zone. Ilmenite crystals from the Panzhihua intrusion may have undergone extensive modification of transition elements during subsolidus re-equilibration with magnetite, leading to the decoupled variations of transition elements in ilmenite across the Lower Zone stratigraphy. Our study indicates that systematic trace element variations of the main cumulus mineral assemblage, rather than a single mineral, need to be considered to better constrain the magmatic differentiation and elemental fractionation of layered intrusions.

Keywords: Mineral trace element geochemistry, Fe-Ti oxides, co-crystallization, Panzhihua layered intrusion, Emeishan large igneous province

Introduction

Layered mafic intrusions provide important insights into magmatic fractionation and crystal accumulation processes in magma chambers (Wager and Brown 1967; Cawthorn 1996). Gravitational settling and dynamic sorting may result in the concentration of denser minerals (e.g., Fe-Ti oxides) in the cumulate rocks relative to lighter ones (e.g., plagioclase), giving rise to different mineral assemblages at different stratigraphic positions in the layered intrusions (Zhang et al. 2012; Maier et al. 2013; Song et al. 2013; Forien et al. 2015). Afterward, compositions of cumulus minerals may be modified by trapped liquids and/or post-cumulus processes (Barnes 1986; Godel et al. 2011; Tanner et al. 2014). Thus, it is problematic to quantify the compositional differentiation of silicate magmas and partitioning of trace elements among co-crystallizing minerals (e.g., Tribuzio et al. 1999; Jang and Naslund 2001; Cawthorn 2007; Jourdan et al. 2007; Jakobsen et al. 2010). Long-standing issues regarding the petrogenesis of layered intrusions, e.g., the nature and evolution of the parental magmas in the Sept Iles layered intrusion (Namur et al. 2010) and the Bushveld Complex (Maier et al. 2013; Tanner et al. 2014), are still hot debated.

Recently, laser ablation-inductively coupled plasma-mass spectrometry (LA-ICP-MS) has made it possible to accurately determine in situ the trace element concentration of small volumes of cumulus minerals (e.g., Liu et al. 2008; Dare et al. 2012). LA-ICP-MS data have been used to elucidate igneous processes, including fractional crystallization (Arndt et al. 2005; Godel et al. 2011; Dare et al. 2014; Liu et al. 2015), and magma replenishment and mixing (Vantongeren and Mathez 2013; Luan et al. 2014; She et al. 2014, 2015), and reactions between cumulate minerals and intercumulus liquid (Cawthorn 2013; Egorova and Latypov 2013; Tanner et al. 2014). However, the critical factors controlling the partitioning of trace elements among cumulus minerals are yet to be well constrained in layered intrusions, and are the focus of this study.

The Permian Panzhihua layered intrusion is a representative mafic-ultramafic igneous complex in the central part of the Emeishan Large Igneous Province (ELIP), SW China. Unusually thick, stratiform massive Fe-Ti oxides (up to 60 m) and magnetite gabbro layers occur in its lower section (Panxi Geological Unit 1984). Although numerous studies were conducted on the origin

* E-mail: songxieyan@vip.gyig.ac.cn

0003-004X/17/0005–1006$05.00/DOI: http://dx.doi.org/10.2138/am-2017-5804

of the Panzhihua Fe-Ti oxide orebodies (e.g., Zhou et al. 2005; Zhang et al. 2007; Ganino et al. 2008; Pang et al. 2008a, 2008b, 2009; Howarth and Prevec 2013; Song et al. 2013; Xing et al. 2014), the fundamental magmatic processes, including magmatic fractionation at depth, co-crystallization of cumulus minerals, and trapped liquid effects, are still poorly understood. In this work, we report a detailed study of trace element variations within magnetite, ilmenite, and clinopyroxene for the Panzhihua intrusion and discuss their implications for magmatic processes and petrogenesis of the Panzhihua massive Fe-Ti oxides, magnetite gabbros, and gabbros.

Geological background

The ELIP is located in the southwestern part of the Yangtze Block, SW China, which consists of a Mesoproterozoic basement overlain by Neoproterozoic to Cenozoic sedimentary cover (Fig. 1a; Zhou et al. 2002). The ELIP contains mainly the Emeishan continental flood basalts, with minor picrite, tephrite, and basaltic andesite, and the genetically related mafic-ultramafic layered intrusions and alkaline felsic plutons (Fig. 1b; Song et al. 2001, 2008; Xu et al. 2001, 2004; Ali et al. 2005; Zhang et al. 2006). The ELIP is believed to have formed from the end of the Guadalupian (~260 Ma) mantle plume (Chung and Jahn 1995; Song et al. 2001, 2004; Zhou et al. 2002).

Several mafic-ultramafic layered intrusions hosting giant Fe-Ti-V oxide deposits, including the Panzhihua, Hongge, Taihe, and Baima layered intrusion, occur in the central part of the ELIP along the N-S trending Panzhihua- and Anninghe faults (Fig. 1b; Panxi Geological Unit 1984; Zhang et al. 1988). SHRIMP zircon U-Pb age dating indicates that these intrusions formed between ~259–263 Ma (Zhou et al. 2002, 2008; Zhong and Zhu 2006; Zhong et al. 2011; Shellnutt et al. 2012; She et al. 2014). These layered intrusions are remarkable because they exhibit clear cyclical variations in mineral abundances, with mafic silicates + Fe-Ti oxides decreasing upward and plagioclase increasing upward. The Panzhihua and Baima intrusions are dominated by magnetite- and apatite-bearing gabbros or troctolite (Zhou et al. 2005; Pang et al. 2008a, 2008b; Zhang et al. 2012; Song et al. 2013; Liu et al. 2014), and the Hongge and Taihe intrusions contain olivine-clinopyroxenite and gabbro (Zhong et al. 2002;

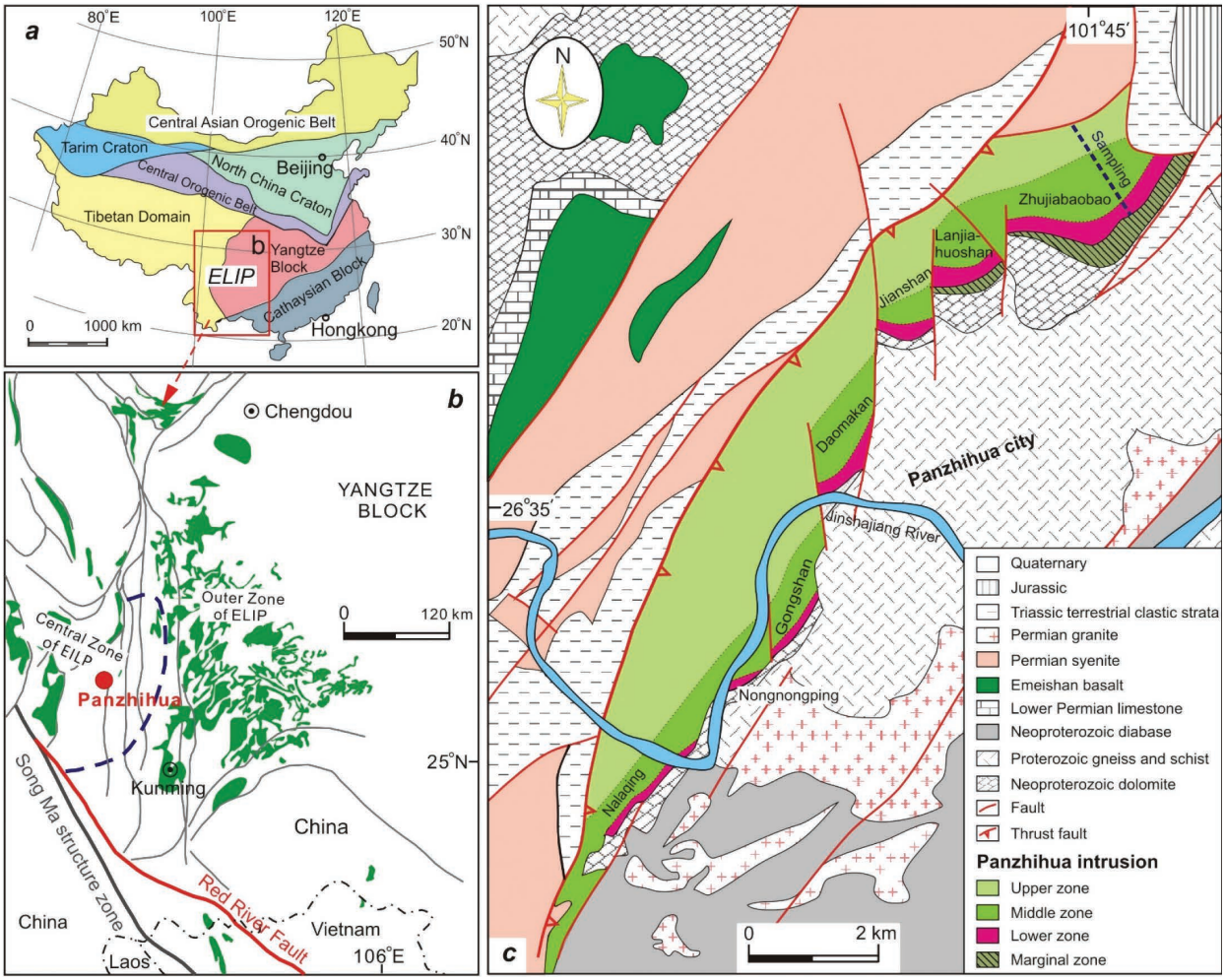

Figure 1. (**a**) Major tectonic units of China (after Song et al. 2008). (**b**) Regional geological map of the Emeishan large igneous province, showing the distribution of the Emeishan continental flood basalts and location of the Panzhihua layered intrusion (modified after Song et al. 2001, 2008). (**c**) Geological map of the Panzhihua intrusion (modified after Panxi Geological Unit 1984 and Song et al. 2001, 2013).

Bai et al. 2012, 2016; Luan et al. 2014; She et al. 2014). Thick stratiform Fe-Ti oxide layers are hosted in the lower and/or middle zones of these intrusions (Panxi Geological Unit 1984).

Geology and petrography

The Panzhihua layered intrusion (263 ± 3 Ma, Zhou et al. 2005) is a sill-like body (~19 km long and ~0.1–2 km thick, with an outcrop area of ~30 km^2) that strikes NE–SW and dips 40–60° to northwest. It is an elongated body that intruded into the Upper Neoproterozoic dolomitic limestone, schist, and gneiss. Apatite gabbro in Upper Zone is in faulted contact with Permian syenites and Triassic shales and coal formations (Fig. 1c; Panxi Geological Unit 1984). The intrusion has been divided into seven segments by a series of N-S-trending strike-slip faults as shown in Figure 1c (Song et al. 2013).

The Panzhihua intrusion can be divided according to mineral assemblage and rock texture into a Marginal Zone at the base, overlain by a Lower Zone, Middle Zone, and Upper Zone (Table 1; Fig. 1c). These divisions are after Song et al. (2013) and Panxi Geological Unit (1984), and correspond to the Marginal Zone, Lower Zone, Middle Zone (a) and Middle Zone (b) of Pang et al. (2008b), respectively. The Marginal Zone is dominated by microgabbro, which is mainly composed of fine-grained clinopyroxene and plagioclase with minor hornblende, magnetite, ilmenite, and olivine (Zhou et al. 2005).

Lower Zone

The Lower Zone is further subdivided into five cyclic units, from Units I to V with decreasing Fe-Ti oxide contents from the base to the top of each unit (Song et al. 2013). Unit I consists of coarse-grained magnetite gabbro and gabbro. Units II to V are characterized by thick massive Fe-Ti oxide layers (~40–60 meters) overlain by medium-grained magnetite gabbros and/or gabbros. Thin layers of magnetite gabbro also occur within the massive Fe-Ti oxide ore layers (Fig. 2a). The massive Fe-Ti oxide ore layers are marked by high Fe-Ti oxide contents (>50 modal% magnetite and 10% ilmenite; the modal abundances of minerals were qualitatively estimated in thin section by Song et al. 2013) and low silicate abundance (<40%, clinopyroxene + plagioclase ± olivine) and 1–4% sulfide contents (pyrrhotite and chalcopyrite, with minor pentlandite, Fig. 2b). The magnetite gabbros contain low abundances of cumulus Fe-Ti oxides (30–45% magnetite and 5–10% ilmenite) but high silicate contents (20–30% clinopyroxene, <20–30% plagioclase, with minor olivine and hornblende), together with 1–3% sulfides (Figs. 2c–2d). In the massive oxide layers and magnetite gabbros, most of the ilmenite crystals are in contact with magnetite, whereas, in some magnetite gabbros, a few ilmenite crystals are separated from magnetite by silicates. Contacts between magnetite and ilmenite are straight to slightly curved and commonly show ~120° triple junctions (Fig. 2b). Some plagioclase crystals show ductile deformed (bent) twins and have thin rims of brown hornblende (Figs. 2c–2d). Most clinopyroxene crystals contain small and lineated platy Fe–Ti oxides inclusions (Figs. 2c–2d), and a few clinopyroxene grains display clear overgrowth rims and anhedral hornblende rims (Fig. 2d). At the top of these cyclic units, the gabbros are distinguished by the lowest contents of interstitial Fe-Ti oxides (<30%), and the highest contents of plagioclase (~30–45%) and clinopyroxene (~30–40%). Furthermore, the magnetite/ilmenite (Mt/Ilm) ratios of this zone generally decrease from the base (4.6–9.3) to the top (3.0–4.4) for each cyclic unit.

Middle Zone

The Middle Zone is subdivided into six cyclic units from VI to XI upward based on lithological variations (Song et al. 2013). Each cyclic unit is marked by magnetite gabbro at the base, and gabbro at the top with decreasing Fe-Ti oxide contents. The magnetite gabbros in these cyclic units have lower Fe-Ti oxides (~30–45%) and higher plagioclase (~25–40%) contents than those of the Lower Zone (Fig. 2e). The mineral assemblage of the Middle Zone gabbro is identical to that of the Lower Zone, containing 20–35% Fe-Ti oxides, 30–45% plagioclase, and 25–40% clinopyroxene. Subhedral to euhedral magnetite and ilmenite grains are mainly separated by silicate minerals. The magnetite gabbros and gabbros in the Middle Zone are generally lower in Mt/Ilm ratios (1.5–4) than those in the Lower Zone (Mt/Ilm = 3.0–9.3). Compared to silicates in the Lower Zone, most clinopyroxene and plagioclase in the

Table 1. Magmatic stratigraphy of the Panzhihua layered intrusion, the Emeishan large igneous province

Characterization	Remarkable features	References
Upper Zone		
Defined by the abrupt appearance of cumulus apatite. The Upper Zone is dominated by apatite gabbro, which is made up of plagioclase (An = 23.5–53.3%), clinopyroxene (Mg# = 51.3–74.8%), magnetite, ilmenite, and minor olivine (Fo = 27.7–64.5%) and apatite.	Free of Fe-Ti oxide ores. Low magnetite/ilmenite ratios.	Panxi Geological Unit 1984; Pang et al. 2009; Song et al. 2013; this study
Middle Zone		
Marked by magnetite gabbros without massive Fe-Ti oxide layers at base, overlain by gabbros. The mineral assemblages are similar to the Lower Zone, but are high proportions of plagioclase (An = 51.8–69.7%), clinopyroxene (Mg# = 70.4– 78.6%), and low abundances of magnetite, ilmenite, olivine (Fo = 65.4–82.3%) and hornblende without sulfides.	Some magnetite gabbro horizons are mined for Fe and Ti. Moderate magnetite/ilmenite ratios.	Panxi Geological Unit 1984; Zhou et al. 2005; Pang et al. 2009; Song et al. 2013; Zhang et al. 2011; This study
Lower Zone		
Marked by massive Fe-Ti oxide layers. The Lower Zone consists of Fe-Ti oxide layers, magnetite gabbros and gabrros, containing magnetite, ilmenite, plagioclase (An = 57.5–62.5%), clinopyroxene (Mg# = 72.0–79.2%), and minor olivine (Fo = 64.4–80.7%), hornblende and sulfides.	Several thick stratiform Fe-Ti oxide layers and magnetite gabbros horizons are mined for Fe, Ti, and V. High magnetite/ilmenite ratios.	Panxi Geological Unit 1984; Zhou et al 2005; Pang et al. 2009; Song et al. 2013; Zhang et al. 2011; This study
Marginal Zone		
The Marginal Zone is composed of micrograbbroic rocks and is proposed to be the chilled base of the intrusion. The mineral assemblages are fine-grained plagioclase (An = 49.6–72.1%), clinopyroxene (Mg# = 80.3–84.6%), hornblende, magnetite, ilmenite, and minor olivine (Fo = 77.9–81.1%) and apatite.	No economic horizons of Fe, Ti, and V. Fine-grained texture of minerals.	Zhou et al. 2005; Pang et al. 2009

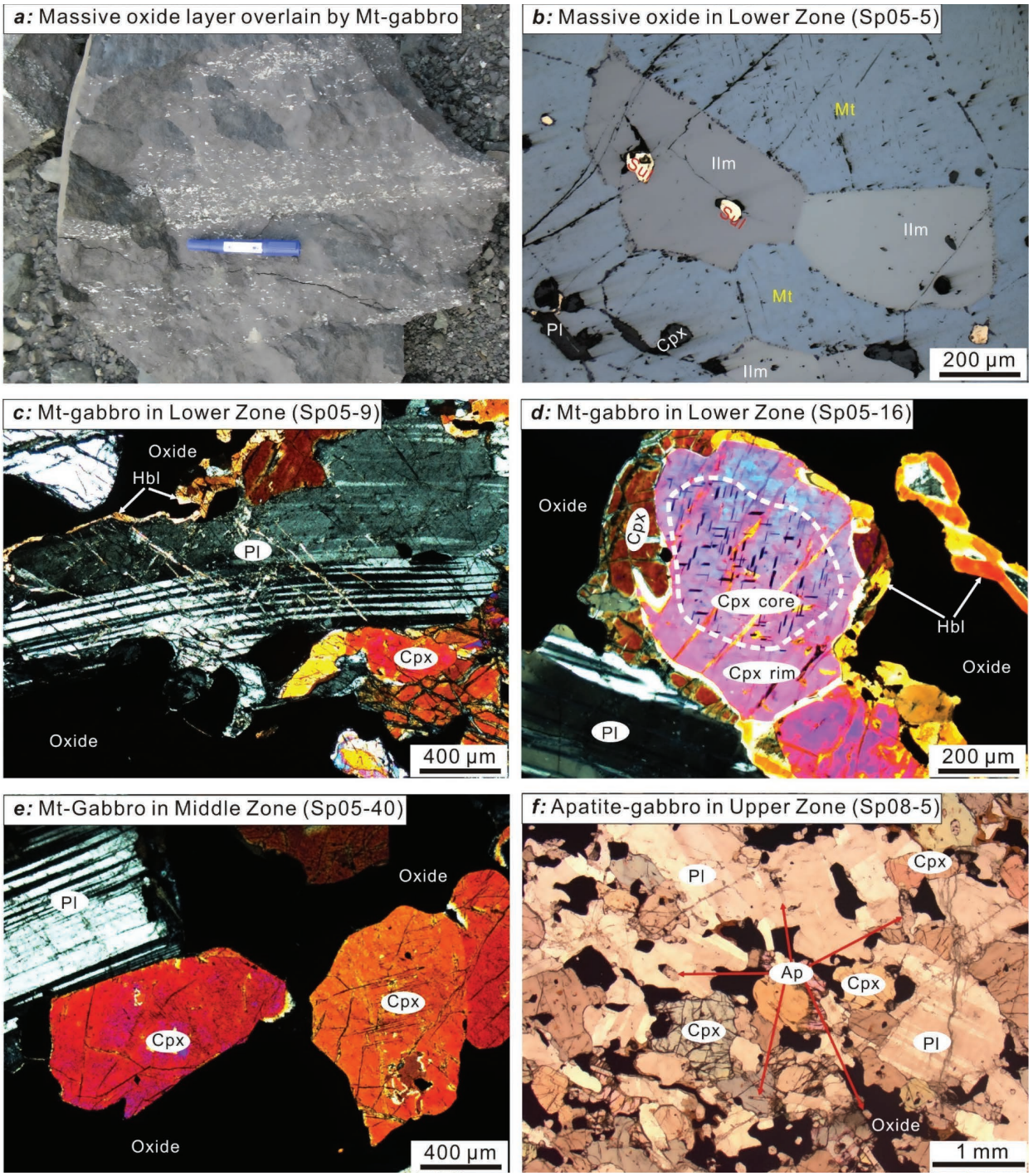

FIGURE 2. Structures and microtextures of the Panzhihua rocks. (**a**) Massive Fe-Ti oxide layers overlain by magnetite gabbro interlayers. (**b**) Polygonal magnetite and ilmenite with straight to slightly curved boundaries and (occasionally) 120° triple junctions in massive Fe-Ti oxide ores. Tiny primary sulfides (mainly pyrrhotite and chalcopyrite) were included in Fe-Ti oxides. (**c**) Magnetite gabbro (Lower Zone) with a bent plagioclase crystal rimmed by anhedral hornblende. (**d**) Two sets of exsolution magnetite lamellae in clinopyroxene (parallel to prismatic cleavage in clinopyroxene) with an overgrowth rim and anhedral hornblende rims (Lower Zone). (**e**) Magnetite gabbro (Middle Zone) with regular and linear boundaries between clinopyroxene and plagioclase with rare hornblende rims. (**f**) Apatite gabbro (Upper Zone) with fine-grained euhedral apatite inclusions in clinopyroxene and plagioclase, and disseminated Fe-Ti oxides among silicates. Cpx = clinopyroxene; Pl= plagioclase; Mt = magnetite; Ilm = ilmenite; Ap = apatite; Oxide = magnetite and ilmenite.

Middle Zone magnetite gabbros and gabbros display more regular and linear edges with rare overgrowth rims or anhedral hornblende rims (Fig. 2e).

Upper Zone

The Upper Zone is characterized by the abrupt appearance of apatite gabbro, which contains <10% Fe-Ti oxides (rarely up to 15%), 50–65% plagioclase, 20–35% clinopyroxene, and ~3–5% apatite (Fig. 2f). Apatite occurs as small euhedral hexagonal crystals enclosed within plagioclase and clinopyroxene, or euhedral to subhedral grains intergrown among silicates and Fe-Ti oxides (Fig. 2f). Subhedral to euhedral magnetite and ilmenite grains are sparse usually separated by silicates. Furthermore, the Upper Zone rocks contain lower Mt/Ilm values (0.8–3) than the magnetite gabbros and gabbros in the Lower and Middle Zones (Pang et al. 2008a; Howarth et al. 2013; Song et al. 2013).

Sampling and Analytical Methods

Fifty-two samples across the whole lithostratigraphic section (except the Marginal Zone) were collected from the Zhujiabaobao open-pit mine, where the Lower and Middle Zones are the thickest and most well exposed (Fig. 1c). Polished thin sections of these rocks were prepared for in situ elemental analyses.

Major and trace element abundances of magnetite, ilmenite, and clinopyroxene were determined in situ by LA-ICP-MS at the State Key Laboratory of Ore Deposit Geochemistry, Institute of Geochemistry, Chinese Academy of Sciences, using an Agilent 7700cs quadrupole ICP-MS coupled to a GeoLasPro 193 nm laser ablation system. The operating conditions and procedures were described in detail by Dare et al. (2012) and Liu et al. (2008) and are summarized as follows: laser beam diameter: 60 μm (for Fe-Ti oxides, BC-28, and GSE-1G) or 44 μm (for clinopyroxene, BHVO-2G, NIST610, BIR-1G, and BCR-2G); laser pulse rate: 6 Hz; laser beam fluence: ~10 J/cm^2 at the sample. Pure He was used as the carrier gas to pass the ablation point within the cell, and mixed with Ar for improving efficiency for aerosol transport. The total acquisition time for each analysis was 90 s (s), including 30 s blank measurement (laser off) and 60 s analysis (laser on). In this study, only the cores of cumulus minerals were ablated and analyzed. Both fine-grained exsolution lamellae (e.g., ilmenite, spinel, and magnetite) and the mineral host (e.g., magnetite, ilmenite, and clinopyroxene) were ablated because the diameter of the laser beam (44 or 60 μm) is larger than the width of the exsolution lamellaes (<20 μm, mostly <10 μm). Therefore, the analytical results represent the initial compositions of magnetite, ilmenite, and clinopyroxene prior to subsolidus exsolution (Dare et al. 2012).

International reference standards GSE-1G and NIST610 were analyzed after every eight analyses for Fe-Ti oxides and clinopyroxene, respectively, to monitor drift in sensitivities. The in-house magnetite standard BC-28 (a massive magnetite from the Bushveld complex, Barnes et al. 2004; Dare et al. 2012, 2014) and international reference materials KL2-G and ML3B-G were measured as unknowns to monitor the data quality of Fe-Ti oxides and clinopyroxene, respectively. Data reduction of Fe–Ti oxides was conducted with the software Igor-pro (http://www.wavemetrics.com) using Fe as the internal standard (see the Fe contents of magnetite in Song et al. 2013 and ilmenite in Zheng et al. 2014 as determined by electron microprobe). Data reduction of clinopyroxene was performed with ICPMSDataCal using BHVO-2G, NIST610, BIR-1G, and BCR-2G as external standards without internal standardization (Liu et al. 2008), because clinopyroxene often hosts small Fe-Ti oxides inclusions as mentioned above. Detection limits for the Fe-Ti oxides and clinopyroxene were 0.1–4.4 and 0.01–1 ppm, respectively. Analytical results of BC-28, KL2-G, and ML3B-G are consistent with their preferred values (Fig. 3, Supplemental[1] Table S1). Major and trace element data of the Panzhihua magnetite, ilmenite, and clinopyroxene are given in Supplemental[1] Tables S2, S3, and S4, respectively. (Throughout paper, deposit tables denoted with S and available online[1].)

Results

Stratigraphic variations

Stratigraphic variations of several selected trace elements and MgO [or Mg#, where Mg# = 100·MgO/(MgO+FeO$_{(T)}$, molar)] in magnetite, ilmenite, and clinopyroxene are illustrated in Figure 4.

The variations in transition metal contents (e.g., Cr, V, Ni, and Sc) in the Lower Zone (Fig. 4) show that the average Cr and Ni contents of magnetite decrease upward in several cyclic units. For example, in Unit V, Cr varies from 490 to 35 ppm, and Ni from 47 to 19 ppm. Similarly, V and Sc concentrations in magnetite decrease upward in each of these cyclic units. The magnetite within Unit I has the lowest Cr (7.2–10.1 ppm) and Ni (9.1–12.3 ppm) contents than any of the other units. Stratigraphic variations of Cr, Ni, V, and Sc in clinopyroxene are similar to those in magnetite. Average Ni and Sc contents in ilmenite decrease upward, but the variations of Cr and V in ilmenite display no clear trends (Fig. 4). It is noteworthy that the high field strength element (HFSE, e.g., Zr, Hf, Nb, and Ta) and rare earth element (REE,

[1]Deposit item AM-17-55804, Supplemental Tables. Deposit items are free to all readers and found on the MSA web site, via the specific issue's Table of Contents (go to http://www.minsocam.org/MSA/AmMin/TOC/2017/May2017_data/May2017_data.html).

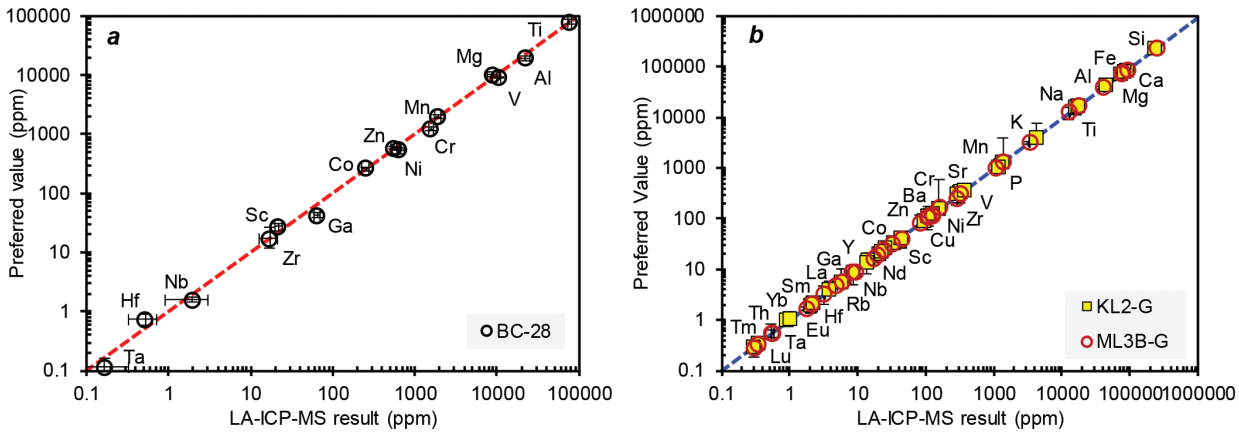

Figure 3. Comparison of LA-ICP-MS analytical results for (**a**) in-house magnetite standard (BC-28; from the Bushveld Complex) and (**b**) international reference materials (KL2-G and ML3B-G) with their preferred values. The preferred values of BC-28 are from Barnes et al. (2004) and Dare et al. (2012, 2014) and those of KL2-G and ML3B-G are from the "GeoREM database" (http://georem.mpch-mainz.gwdg.de/sample_query_pref.asp).

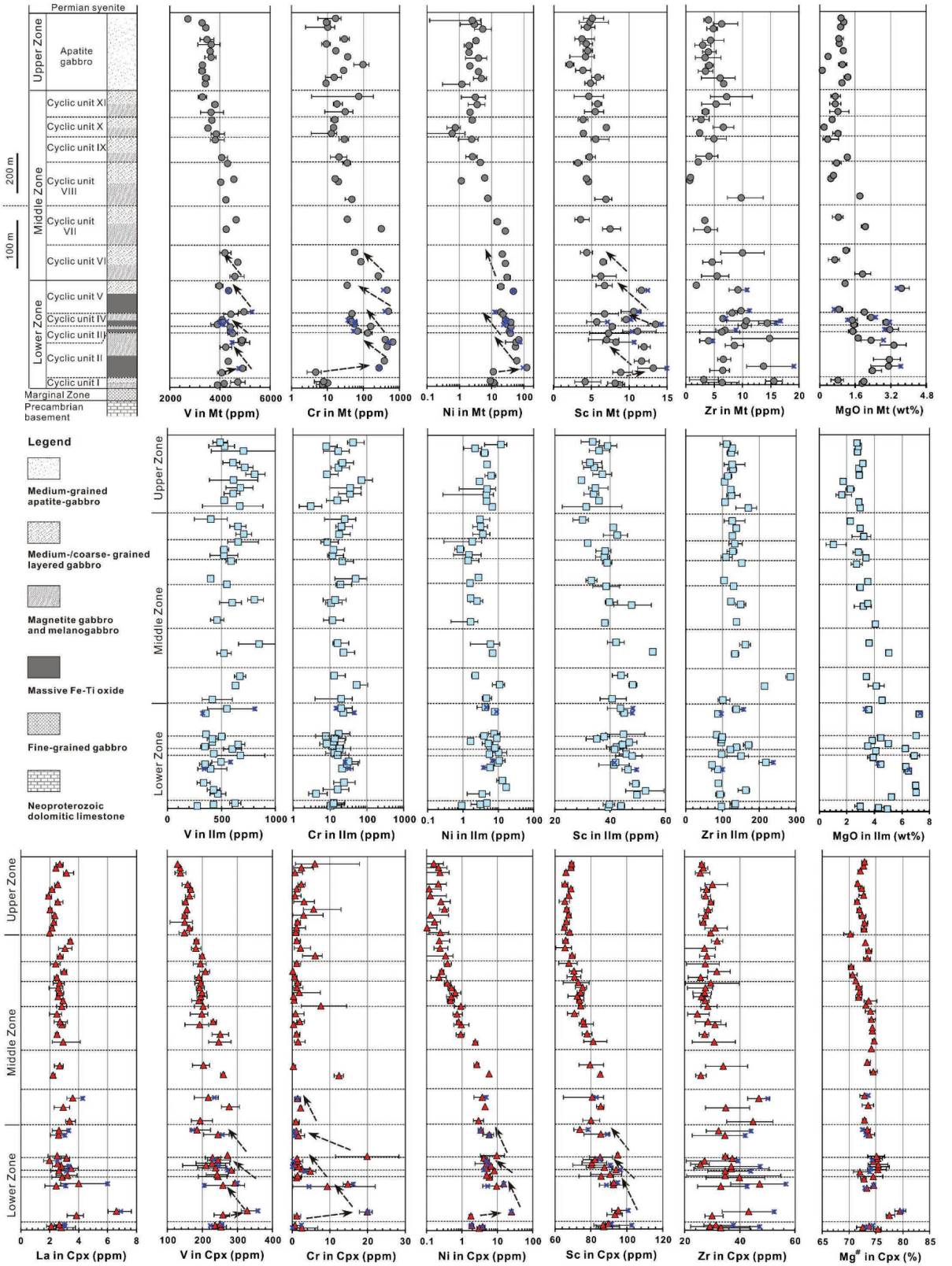

FIGURE 4. Variations of key trace elements and MgO (or Mg#) in magnetite, ilmenite, and clinopyroxene with relative stratigraphic position of the Panzhihua intrusion. Filled symbols are average contents of these elements, and error bars represent the range measured in this study. Blue crosses mean the mineral grains in contact with anhedral hornblende rims.

e.g., La) concentrations in the Fe-Ti oxides and clinopyroxene in the Lower Zone are more variable than those in the Middle and Upper Zones (Fig. 4). Magnetite and clinopyroxene crystals in contact with anhedral hornblende have higher HFSE and REE than those not in contact with anhedral hornblende (Fig. 4, Tables S2 and S4). In addition, ilmenite in contact with silicates in the magnetite gabbros contains higher Cr, V, and Co than those in contact with magnetite (Table S3). Both magnetite and ilmenite contain variable MgO contents from 0.82 to 3.68 wt% and from 2.95 to 7.25 wt%, respectively, while clinopyroxene has a small range of Mg# values (72.0–79.4%, Fig. 4).

Magnetite and clinopyroxene in the Middle Zone show more regular changes and smaller cyclic variations in trace element concentrations than those in the Lower Zone (Fig. 4). Transition metals in magnetite and clinopyroxene decrease up stratigraphy in the Middle Zone. Both the magnetite and clinopyroxene in the Middle Zone contain not only lower abundances of compatible elements (e.g., V and Cr), but also slightly lower incompatible element contents (e.g., Zr and La) than those in the Lower Zone (Fig. 4). Ilmenite in the Middle Zone has smaller variations in both major and trace element concentrations, and has slightly higher V contents than that in the Lower Zone (Fig. 4). In addition, magnetite and ilmenite in the Middle Zone are lower in MgO than those in the Lower Zone, decreasing up the stratigraphic column from 1.93 to 0.20 wt% and from 4.56 to 1.00 wt%, respectively (Fig. 4). Clinopyroxene in the Middle Zone has slightly lower Mg# (70.3–74.6%) than that in the Lower Zone (Fig. 4).

In the Upper Zone, the Fe-Ti oxides and clinopyroxene are characterized by relatively small stratigraphic variations in most trace element and MgO (or Mg#) concentrations (Fig. 4). Both magnetite and clinopyroxene crystals from the Upper Zone contain significantly lower contents of transition metal contents (e.g., Cr, V, Ni, and Sc) than from the Lower and Middle Zones (Fig. 4). By contrast, the abundances of HFSE and REE, such as Zr and La, in the magnetite and clinopyroxene crystals of this zone are generally comparable to those of the Middle Zone, but lower than those of the Lower Zone (Fig. 4).

Multi-element variation patterns

Multi-element spider diagrams are used to compare the full suite of elemental concentrations in the Fe-Ti oxides and clinopyroxene (Figs. 5–7). Both trace and major elements from the Panzhihua magnetite are normalized to the Emeishan high-Ti picrite that was proposed to be compositionally similar to the primary magmas of the layered intrusions (Kamenetsky et al. 2012; Hou et al. 2013; Song et al. 2013) and are plotted in order of increasing compatibility with magnetite (Dare et al. 2012, 2014) (Fig. 5). The magnetite shows strong negative Ni, Co, Mg, and Sc anomalies and V, Zn, and Ga enrichments (Fig. 5). The multi-element patterns of the Panzhihua magnetite resemble the basal magnetite of the Upper Zone magnetite layers

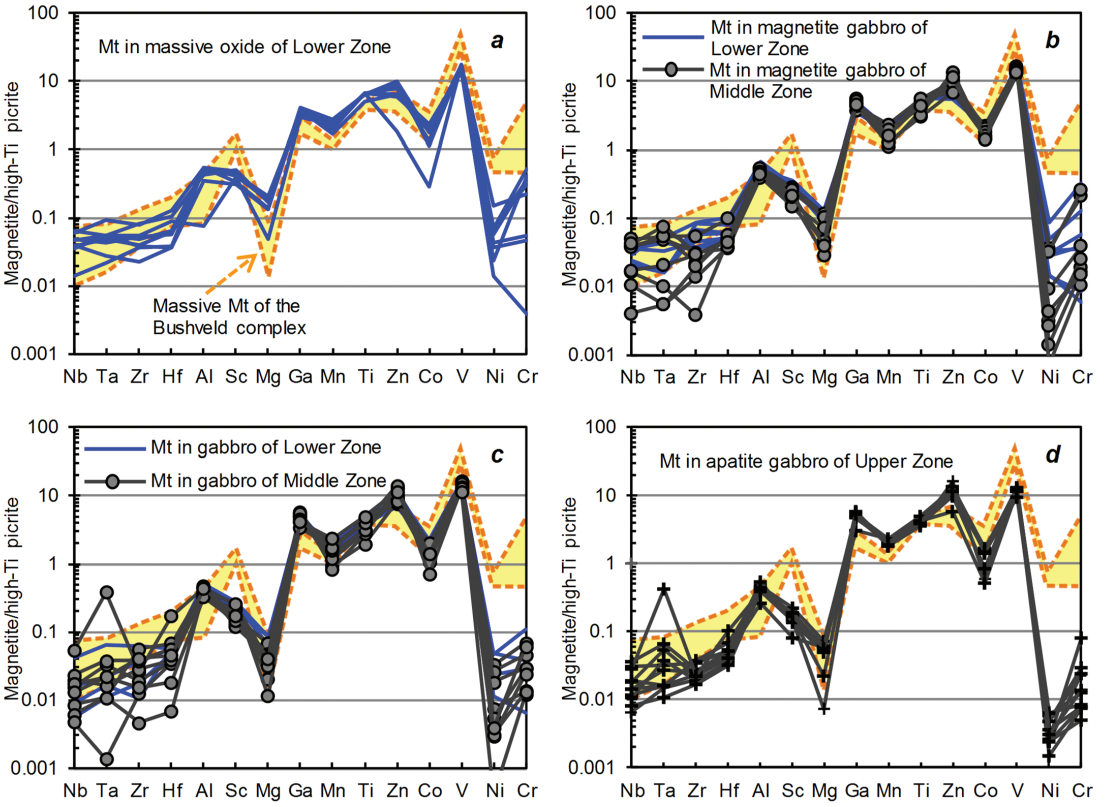

FIGURE 5. Emeishan high-Ti picrite normalized multi-element diagrams for Panzhihua magnetite (in increasing order of trace element compatibility with magnetite, after Dare et al. 2012, 2014). Magmatic magnetite from the Bushveld Complex (light yellow field, data from Dare et al. 2014) is plotted for comparison. The Emeishan high-Ti picrite data are from Kamenetsky et al. (2012).

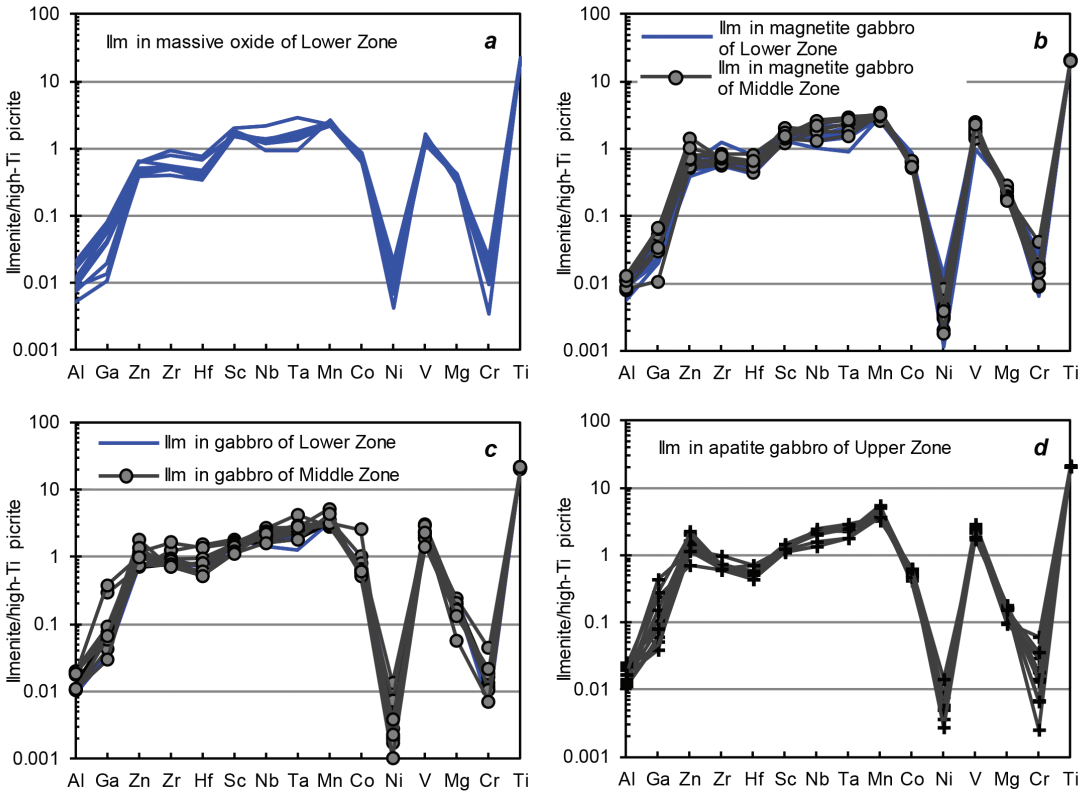

FIGURE 6. Emeishan high-Ti picrite normalized multi-element diagrams for Panzhihua ilmenite (in increasing order of trace element compatibility with ilmenite, after Jang and Naslund 2003; van Kan Parker et al. 2011; Dygert et al. 2013). The Emeishan high-Ti picrite data are from Kamenetsky et al. (2012).

in the Bushveld Complex (Dare et al. 2014), except the latter is relatively enriched in Sc, V, Ni, and Cr (Fig. 5). In addition, the Panzhihua magnetite becomes increasingly depleted in Ni, Cr, Co, Mg, and Sc from the Lower Zone massive Fe-Ti oxide layers, through the Lower and Middle Zone magnetite gabbros and gabbros to the Upper Zone apatite gabbro (Fig. 5).

Eleven trace elements and four major elements of ilmenite are plotted in order of increasing compatibility (Jang and Naslund 2003; van Kan Parker et al. 2011; Dygert et al. 2013) (Fig. 6). When normalized to the Emeishan high-Ti picrite (Kamenetsky et al. 2012), the Panzhihua ilmenite has similar patterns with significant Al, Ga, Co, Ni, Mg, and Cr depletions and slight Mn, V, and Ti enrichments (Fig. 6). Geochemical variations of the transition elements (e.g., V, Co, and Ni) in all ilmenite crystals are very small, whereas variations of Nb and Hf are large (27.3–79.5 and 1.5–6.7 ppm, respectively; Fig. 6).

The Panzhihua clinopyroxene trace element patterns normalized to the average composition of clinopyroxene phenocrysts in the Emeishan high-Ti picrite (Kamenetsky et al. 2012) are plotted in the order of increasing compatibility (Dygert et al. 2014). The clinopyroxene trace element patterns are generally flat with negative Ti, V, and Sc anomalies (Fig. 7). These negative anomalies become more distinct from the Lower Zone massive Fe-Ti oxide layers, through the Lower and Middle Zone magnetite gabbros and gabbros to the Upper Zone apatite gabbro. Except for the clinopyroxene in the Lower Zone Fe-Ti massive oxide layers, most clinopyroxene in the magnetite gabbros and gabbros and apatite gabbro are weakly depleted in Nb and Hf (Fig. 7).

DISCUSSION

The trace element concentrations in cumulus minerals depend primarily on the following factors: (1) composition of the parental magmas, (2) fractional crystallization, and (3) their partition coefficients (Dare et al. 2014 and references therein). Furthermore, their compositions may also be modified by trapped intercumulus liquids (Barnes 1986; Godel et al. 2011) and/or diffusive interchange between adjacent crystals or fluids (e.g., Tanner et al. 2014). As mentioned above, the Panzhihua Lower and Middle Zones are dominated by massive Fe-Ti oxide ores, magnetite gabbros, and gabbros, which are composed of magnetite, ilmenite, clinopyroxene, plagioclase, and minor olivine, whereas the Upper Zone apatite gabbro is rich in cumulus apatite. Song et al. (2013) proposed that the Panzhihua magnetite and ilmenite co-crystallized with clinopyroxene, after the crystallization of olivine and plagioclase. In the following sections, we discuss the main processes and factors that control the partitioning of trace elements into the Panzhihua Fe-Ti oxides and clinopyroxene based on the concentrations and correlations of these minerals.

Prior fractionation and sulfide removal at depth

The relatively low forsterite (Fo) values of all olivine crystals (<82.5 mol%) suggest that the Panzhihua parental magma was moderately evolved prior to emplacement (Pang et al. 2009;

Zhang et al. 2011). Moreover, the Panzhihua cumulate rocks are characterized by high Cu/Ni and Pd/Ir ratios (Zhou et al. 2005; Howarth and Prevec 2013). MELTS thermodynamic calculations (Ghiorso and Sack 1995) indicate that the Panzhihua parental magma was generated after fractionating spinel, olivine, and clinopyroxene from a picritic magma in a deep-seated magma chamber (Song et al. 2013). These results demonstrate that the Panzhihua parental magma may have undergone fractionation prior to emplacement. This is further supported by the Panzhihua clinopyroxene compositions, because these minerals (especially those from the Lower Zone rocks) contain higher HFSE and REE than clinopyroxene from the Emeishan high-Ti picrite (Fig. 7a). This implies that the parental magma entering the Panzhihua magma chamber was indeed moderately evolved, as it was more enriched in incompatible elements (i.e., HFSE and REE) than the Emeishan high-Ti picrite.

In the normalized multi-element diagrams, the Panzhihua magnetite and ilmenite display strongly negative Ni and Co anomalies (Figs. 5 and 6). Both Ni and Co are compatible in magnetite and ilmenite (see partition coefficients in Table S5). A potential interpretation for these negative anomalies is in situ sulfide liquid immiscibility along with crystallization of Fe-Ti oxides in the Panzhihua magma chamber, because Ni and Co partition strongly into immiscible sulfide liquids ($D_{Ni}^{Sul/Liq}$ = 500–800, Peach et al. 1990; $D_{Co}^{Sul/Liq}$ = 61–80, Rajamani and Naldrett 1978). However, the high modal of primary sulfide (up to ~4%, pyrrhotite and chalcopyrite, with minor pentlandite; Song et al. 2013), and low Ni contents (<100 ppm) of the Panzhihua cumulate rocks (Zhou et al. 2005; Howarth and Prevec 2013) suggest a weak effect from in situ sulfide immiscibility on the Ni and Co depletions in magnetite and ilmenite.

Alternatively, these negative anomalies may result from Ni and Co depletions in the Panzhihua parental magma. These depletions could be attributed to olivine fractionation ($D_{Ni}^{Ol/Liq}$ = 22.3 ± 9.12, $D_{Co}^{Ol/Liq}$ = 5.2 ± 1.5, Laubier et al. 2014) and/or removal of sulfide liquids at depth. However, MELTS simulations indicated that proportions of crystallized olivine were relatively low (~2.4 wt%) prior to emplacement (Song et al. 2013), and thus olivine fractionation could not be alone responsible for the observed Ni and Co depletions in magnetite and ilmenite. Consequently, Ni and Co depletions of the parental magma are attributed to sulfide segregation and removal at depth. This hypothesis is evidenced by the depletion of platinum group elements and very high Cu/Pd values (>60 000) of the Panzhihua rocks relative to the genetically related Emeishan high-Ti basalts (Howarth and Prevec 2013). In addition, the magnetite and ilmenite in the Middle and Upper Zones are progressively more depleted in Ni and Co than those in the Lower Zone (Figs. 5 and 6), indicating a coupling of sulfide segregation and Fe-Ti oxide crystallization in the Panzhihua magma chamber.

Although Cr is compatible in Fe-Ti oxides ($D_{Cr}^{Mt/Liq}$ = 19.3–340, Dare et al. 2014; $D_{Cr}^{Ilm/Liq}$ = 5.9–22.4, Dygert et al. 2013; Table S5), both magnetite and ilmenite in the Panzhihua intrusion show strong negative Cr anomalies in the multi-element normalized diagrams (Figs. 5 and 6). In addition, magnetite from the Lower Zone rocks contains much lower Cr (~10–450 ppm) than magnetite from the megacyclic Unit I of the Sept Iles layered intrusion, Canada (Cr = 5600–12 300 ppm, Namur et al. 2010). On the

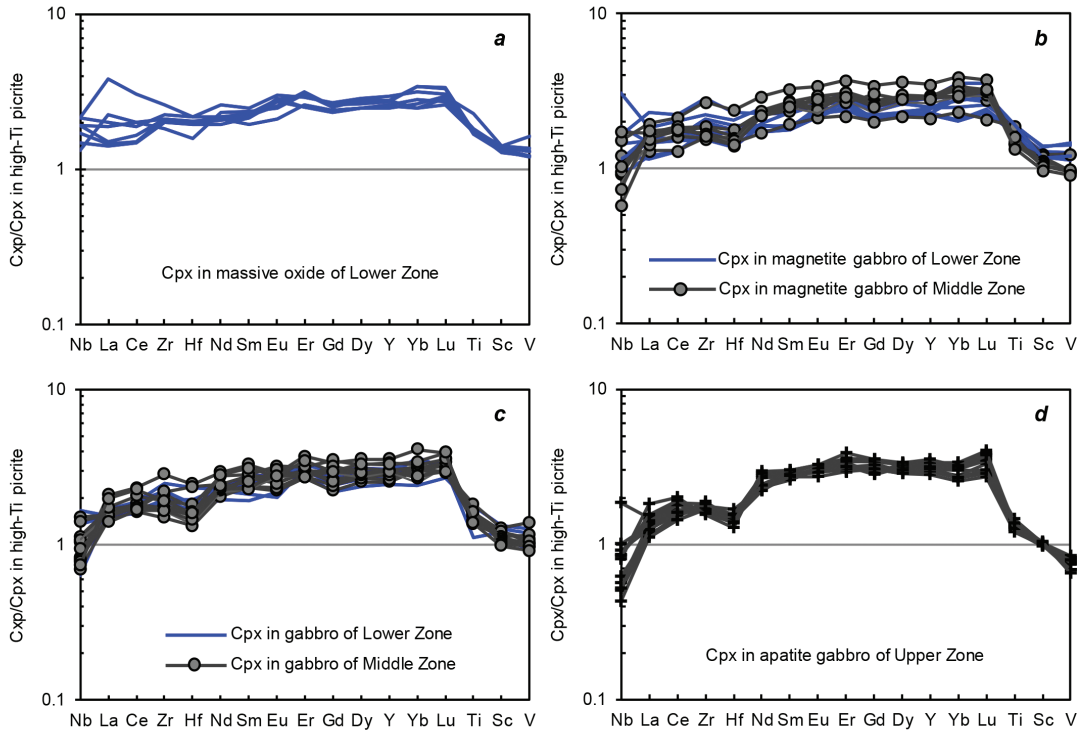

FIGURE 7. Multi-element variation diagrams for Panzhihua clinopyroxene, normalized to the average composition of clinopyroxene phenocrysts in the Emeishan high-Ti picrite (clinopyroxene data are from Kamenetsky et al. 2012).

other hand, the Panzhihua olivine and plagioclase are slightly more primitive ($Fo_{54–82}$, $An_{40–70}$, Pang et al. 2009; Zhang et al. 2011) than their Sept Iles counterparts ($Fo_{50–72}$, $An_{34–69}$, Namur et al. 2010), suggesting that the Panzhihua parental magma was less evolved than that in the Sept Iles intrusion. The significant Cr depletions in the Panzhihua magnetite and ilmenite cannot be ascribed to either silicate fractionation or sulfide removal, because Cr is moderately incompatible or compatible in silicates ($D_{Cr}^{Ol/Liq}$ = 0.63–1.85, Kloeck and Palme 1988; Beattie 1994; $D_{Cr}^{Cpx/Liq}$ = 1.66–3.8, Hart and Dunn 1993; Hauri et al. 1994; $D_{Cr}^{Plagioclase/Liq}$ = 0.019–0.365, Aignertorres et al. 2007; Table[1] S5) and sulfides ($D_{Cr}^{Sul/Liq}$ = 0.9, Pedersen 1979). The bulk partition coefficient of Cr would be slightly incompatible overall if only silicates crystallized. Instead, such depletions most likely reflect early chromite and/or Cr-magnetite fractionation, which would have scavenged Cr to generate the major Cr depletion seen the residual magma and thus in magnetite and ilmenite. The fine-grained chromite/or Cr-magnetite inclusions (Cr_2O_3 = 2.0–10.8 wt%) in olivine from the Lower Zone rocks were thought to be early crystallized and trapped Fe-Ti oxide crystals (Pang et al. 2008a) or xenocrysts (Howarth et al. 2013; Zhou et al. 2013), lending further support to the above interpretation.

Co-crystallization of Fe-Ti oxides and clinopyroxene

At the oxygen fugacity of the quartz-fayalite-magnetite buffer, saturation of Fe-Ti oxides generally occurs during the late stages of fractionation in mafic magmas (i.e., the Fenner trend; Fenner 1929; Wager and Brown 1967; Frost and Lindsley 1991; Toplis and Carroll 1995; Thy et al. 2006). Therefore, Fe-Ti oxide rich layers commonly occur in the upper sections of layered intrusions, such as the Bushveld Complex, and the Skaergaard intrusion (Eales and Cawthorn 1996; Nielsen 2004; Tegner et al. 2006). However, stratiform massive Fe-Ti oxide layers and magnetite gabbros occur in the Lower and Middle Zones at Panzhihua. This feature is also the case for the Sept Iles layered intrusion, where 24 layers of massive Fe-Ti oxide ore (up to 1 m thick) occur in the troctolites of the Layered Series in its lower section. The formation of the Sept Iles Fe-Ti oxide ore layers was attributed to early Fe-Ti oxide saturation together with olivine and plagioclase crystallization from a ferrobasaltic liquid (Namur et al. 2010). Compared to the Sept Iles intrusion, the Panzhihua intrusion was formed from a relatively primitive parental magma, in which magnetite and clinopyroxene crystallized after olivine and plagioclase (Song et al. 2013). This co-crystallization suggests that magnetite, ilmenite, and clinopyroxene could compete for the (more) compatible trace elements.

As mentioned above, the transition metals (e.g., Ni, Cr, and V) are compatible in magnetite, ilmenite, and clinopyroxene (see partition coefficients in Table S5). The strong decreases of Ni, Cr, and V contents in magnetite and clinopyroxene with stratigraphic height within several Lower Zone cyclic units (Fig. 4) reflect a depletion of these elements in the residual liquids in response to early magnetite and clinopyroxene crystallization (i.e., $D_{bulk}^{Ni,Cr,V} > 1$). The repetitive reversals of Ni, Cr, V, and MgO (or Mg#) contents in magnetite and clinopyroxene from the cyclic units of the Panzhihua intrusion indicate multiple magma replenishments (Fig. 4). These reversals are consistent with cyclic variations of chemostratigraphic columns of the Panzhihua whole rocks (Song et al. 2013), and are also similar to the chemostratigraphic variations of the Bushveld complex (Cawthorn 2007; Tanner et al. 2014). Moreover, the positive correlations of Ni, Cr, V, and Sc in the Panzhihua magnetite and clinopyroxene imply that they co-crystallized from the parental magma (Figs. 8a–8d). The Sc concentrations in clinopyroxene from the Lower Zone are higher than those in the Emeishan high-Ti picrite (Fig. 7), demonstrating that the Panzhihua parental magma was not Sc depleted. The increasingly negative Sc anomalies in magnetite from the Lower Zone to the Middle and Upper Zones (Fig. 5) suggest co-crystallization of clinopyroxene and magnetite with increasing proportions of clinopyroxene upward because Sc is preferentially partitioned into clinopyroxene (see partition coefficients in Table S5, the D_{bulk} would be compatible for Sc according to proportions of crystallized minerals proposed by Song et al. 2013). On the other hand, Nb and Ta are compatible and Zr and Hf are moderately incompatible in ilmenite (Dygert et al. 2013), while these elements are highly incompatible for olivine, clinopyroxene, and plagioclase (see partition coefficients in Table S5). The flat normalized multi-element patterns of the Lower Zone clinopyroxene suggest that ilmenite crystallization may not have played a critical role in the partitioning of Nb, Ta, Zr, and Hf into clinopyroxene (Fig. 7a). Magnetite and clinopyroxene (plagioclase as well) were therefore likely major early cumulate phases that fractionated soon after the parental magma entered the Panzhihua magma chamber. The ilmenite in the Lower Zone, however, crystallized from the parental magma somewhat after magnetite and clinopyroxene. Consequently, the Lower Zone magnetite gabbros have lower TiO_2 than the Middle Zone magnetite gabbros with the same $Fe_2O_{3(T)}$ (Zhou et al. 2005; Pang et al. 2008b; Song et al. 2013). Co-crystallization of magnetite and clinopyroxene in this study is inconsistent with the proposed model, which argued that the silicates were not in equilibrium with the Fe-Ti oxides and the massive ores formed without the presence of silicates due to intrusion of H_2O-rich magma (Howarth et al. 2013).

The clinopyroxene in the Middle and Upper Zone rocks is more depleted in Nb, Zr, and Hf than that in the Lower Zone rocks (Fig. 7). These depletions indicate that ilmenite and clinopyroxene co-crystallized, and that the increasing proportion of ilmenite scavenges Nb, Zr, and Hf from the Lower Zone to the Middle and Upper Zones, given that these elements are preferentially partitioned in ilmenite (see partition coefficients in Table S5). This proposal also agrees with the observed decreases in Mt/Ilm ratios upward the section. The positive correlations of Sc and Zr between ilmenite and clinopyroxene from the Middle and Upper Zone rocks (especially gabbros) (Figs. 8d–8e) demonstrate their co-crystallizing relationship. The scattered correlations in Cr and V contents between ilmenite and clinopyroxene (Figs. 8a–8c) may indicate diffusive modification during subsolidus re-equilibration upon cooling (see discussion below). Furthermore, positive correlations of Ni, Cr, V, and Sc between magnetite and clinopyroxene in the Middle and Upper Zone rocks indicate not only a co-crystallizing relationship, but also a decrease of these elements in the residual magma after extensive magnetite, ilmenite, and clinopyroxene fractionation (Figs. 8a–8d).

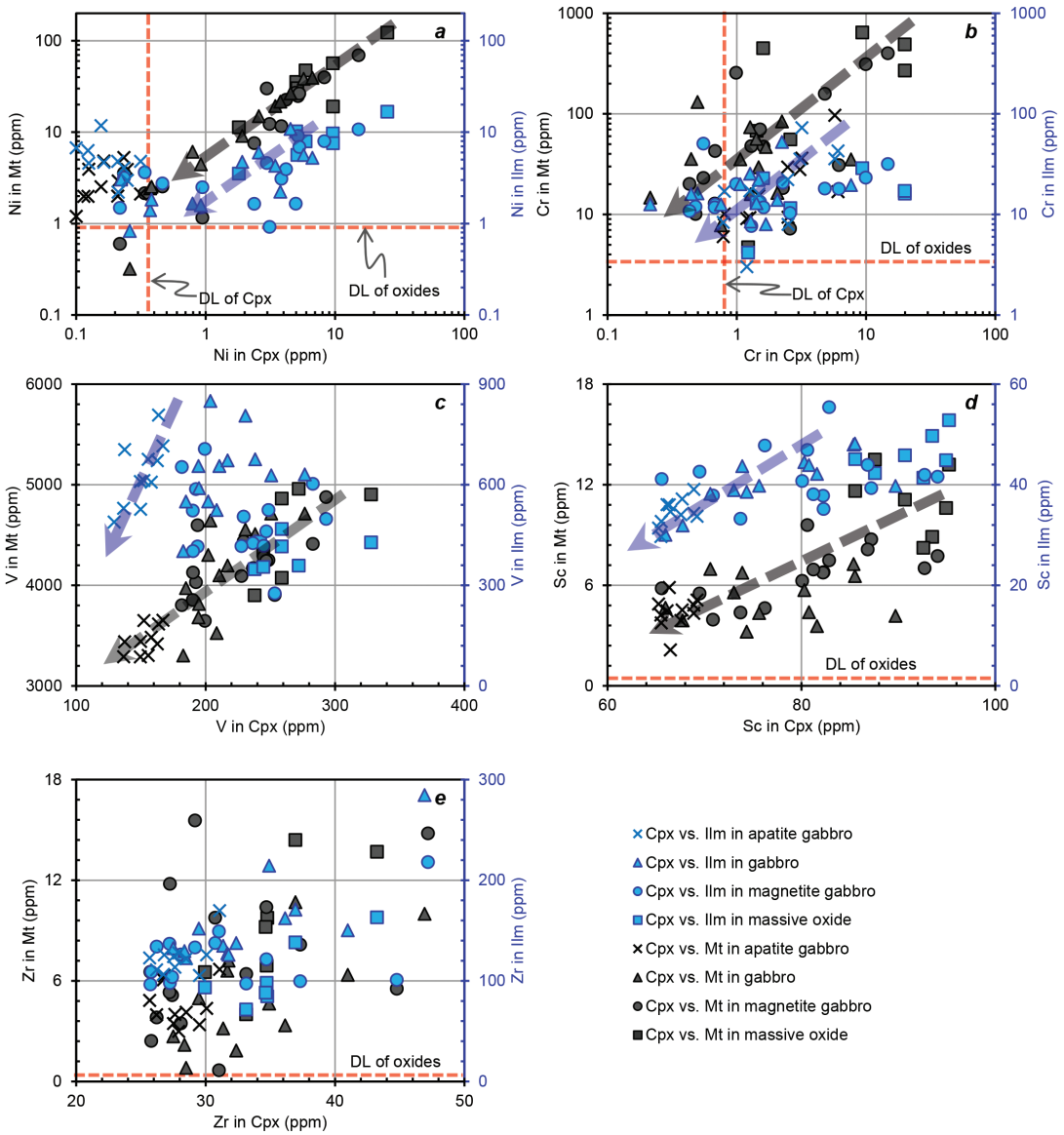

FIGURE 8. Correlation plots for the average contents of (**a**) Ni in clinopyroxene vs. Ni in magnetite and ilmenite (y-axis on the left for magnetite; y-axis on the right for ilmenite); (**b**) Cr in clinopyroxene vs. Cr in magnetite and ilmenite; (**c**) V in clinopyroxene vs. V in magnetite and ilmenite; (**d**) Sc in clinopyroxene vs. Sc in magnetite and ilmenite; and (**e**) Zr in clinopyroxene vs. Zr in magnetite and ilmenite for the different Panzhihua rock types. Abbreviations: Cpx = Clinopyroxene, Mt = Magnetite, Ilm = Ilmenite; DL = Detection Limit.

Trapped liquid shift in the Lower Zone

The concentrations of incompatible trace elements in magnetite and clinopyroxene—particularly the highly incompatible Zr, Nb, and REE—in the Lower Zone (and Unit VI in the Middle Zone) are higher than those in the Middle (Units VII–XI) and Upper Zones (Fig. 4, Tables S2 and S4). This is in contrast to the expected geochemical variations, which would become more enriched up stratigraphy because of their incompatible behavior (e.g., Dare et al. 2014). Moreover, the incompatible element contents in different magnetite (as well as clinopyroxene) grains within a single sample in the Lower Zone are highly heterogeneous compared to those in the Middle and Upper Zones (Fig. 4, Tables S2 and S4). These features are difficult to explain through fractionation alone, and may result from subsequent elemental modification during crystallization of the trapped intercumulus liquids (i.e., trapped liquid shift, Barnes 1986).

The effect of trapped liquids have been widely documented in cumulates from mafic-ultramafic layered intrusions and have been used to interpret mineral compositions in cumulate rocks (e.g., Cawthorn 1996, 2007, 2013; Lundgaard et al. 2006; Egorova and Latypov 2013). Song et al. (2013) estimated that the proportions of trapped liquids in the Panzhihua Lower and Middle Zone rocks were below 5% using whole-rock P concentrations. Similarly, Bai et al. (2014) proposed that less than 5%

of trapped liquids existed in the Panzhihua massive Fe-Ti oxide layers based on whole-rock REE contents. The small percentages of trapped liquids in the Lower Zone indicate that the porosity in these rocks was low, perhaps due to significant compaction by the gravitational settling of Fe-Ti oxides and clinopyroxene during the formation of this zone. This is supported by the ductile deformation (bent) of the plagioclase crystals in the magnetite gabbro (Fig. 2c).

The magnitude of the trapped liquid shift on mineral compositions depends on the amount of trapped liquids, the modal ratios of the cumulus phases, and the partition coefficient for one element (Barnes 1986; Cawthorn 2007). Minor interstitial clinopyroxene and plagioclase, together with hornblende rims around these minerals (Figs. 2b–2d) in the Lower Zone massive Fe-Ti oxide layers and magnetite gabbros, suggest that the modal proportions of trapped liquids were quite low. The trapped liquid would become increasingly enriched in incompatible trace elements with decreasing temperature. Therefore, the incompatible trace element contents of the magnetite and clinopyroxene in contact with intercumulus liquid would be significantly modified by re-equilibration and/or overgrowth. This hypothesis is supported by the observations that the magnetite and clinopyroxene with hornblende rims have higher incompatible trace element contents than those not in contact with hornblende rims (Fig. 4, Tables S2 and S4). Such a "trapped liquid shift" is also recorded by the overgrowth rim of clinopyroxene (Fig. 2d). On the other hand, for the compatible elements (such as Ni, Cr, V, and Sc), this shift could be trivial and ignored in the Lower Zone, because these elements in the intercumulus liquid would be buffered well by magnetite, ilmenite, and clinopyroxene (Cawthorn 2007).

By contrast, trace element abundances in Fe-Ti oxides and clinopyroxene from individual samples within the upper part of Middle (Units VII–XI) and Upper Zones are commonly homogeneous (Fig. 4; Tables S2 and S4). This suggests that the role of trapped liquids on the cumulus minerals in these rocks is insignificant. This hypothesis can be further tested using Ni, Cr, and V contents in the cumulus minerals. For the upper part of the Middle (Units VII–XI) and Upper Zone rocks, the gabbros and apatite gabbros have high proportions of plagioclase (30–65%), in which Ni, Cr, and V are highly incompatible. Since cumulus plagioclase cannot buffer Ni, Cr, and V contents in the intercumulus liquids, the trapped liquid shift would result in much lower concentrations of these elements in clinopyroxene and magnetite than what would be produced during equilibrium crystallization (Cawthorn 2007; Tanner et al. 2014). This expectation is not observed in the stratigraphic variations of trace elements, as magnetite and clinopyroxene do not display abrupt decreases of Ni, Cr, and V contents from the magnetite gabbros to the gabbros and apatite gabbros (Fig. 4), suggesting no extensive trapped liquid shift in these rocks. It was likely that most of the residual liquids were squeezed out of the chamber during the formation of the Middle and Upper Zones (Pang et al. 2009), as evidenced by the homogenous clinopyroxene crystals with rare, late-stage overgrowth rims in these zone rocks (Fig. 2e).

Diffusive modification of transition elements in ilmenite

Unlike magnetite and clinopyroxene, the Panzhihua ilmenite unexpectedly shows decoupled variations in transition elements (e.g., Cr and V) with stratigraphic height in the Lower Zone (Fig. 4). It would be expected decrease upward, due to their compatible behavior, in each cyclic unit. The correlation of Cr contents between ilmenite and clinopyroxene in the Lower Zone is less defined than that between magnetite and clinopyroxene, whereas Cr contents are positively correlated between ilmenite and clinopyroxene in the Middle and Upper Zones (Fig. 8b). Similar correlation of V contents between ilmenite and clinopyroxene is observed in these zones (Fig. 8c). Such compositional variations in the Lower Zone ilmenite are difficult to explain by either prior fractionation at depth, co-crystallization, or trapped liquid shift as discussed above.

An alternative explanation for the decoupled variations of the ilmenite transition elements in the Lower Zone is diffusive modification of these elements between the Fe-Ti oxides during subsolidus re-equilibration. Previous studies have demonstrated that subsolidus re-equilibration involves the exchange of Fe^{3+}, Ti^{4+}, Fe^{2+}, and Mg^{2+} between Fe-Ti oxides (as well as silicates) in layered intrusions (Frost and Lindsley 1991; Pang et al. 2008b). The straight to slightly curved contacts between Panzhihua magnetite and ilmenite crystals indicate that they have undergone significant subsolidus re-equilibration (Fig. 2b). It is thus reasonable to infer that the trace elements may have been redistributed among the Fe-Ti oxides during subsolidus re-equilibration upon cooling. Such redistributions would be controlled by the relative partition coefficients for the different minerals (e.g., $K_{D(Cr,V)}^{Mt/Ilm}$, Tanner et al. 2014). With decreasing temperature, the transition elements diffused from ilmenite into magnetite in which they are more compatible (e.g., $K_{D(Cr,V)}^{Mt/Ilm} > 1$, Table S5). Meanwhile, the diffusive redistributions of the transition elements are affected by relative modal abundances of magnetite and ilmenite in the rocks according to the mass balance relation. In the Lower Zone, magnetite is a dominant mineral in the massive Fe-Ti oxide layers and magnetite gabbros. In these rocks, Cr and V diffusing into magnetite from ilmenite could not significantly modify the primary compositions of magnetite because of high modal abundances of magnetite relative to ilmenite (Mt/Ilm = 3.0–9.3 in the Lower Zone). On the other hand, this diffusive re-equilibration would result in distinct decreases in Cr and V in the ilmenite. Consequently, the magnetite has seen large decreases of Cr and V in the Lower Zone as expected from fractional crystallization, while the ilmenite shows low and constant Cr and V contents in the massive Fe-Ti oxide layers, resulting in weak correlations between magnetite and ilmenite (Fig. 9). These results are consistent with the extensive Fe isotope exchange between magnetite and ilmenite documented in the lower zone of the Baima layered intrusion in the ELIP. Chen et al. (2014) suggested that the magnetite preserved its original magmatic Fe isotope signatures ($\delta^{57}Fe$ = 0.15–0.36‰, in agreement with values of 0.20–0.36 that would be expected for minerals in equilibrium with the parental magma), whereas the ilmenite isotopic compositions ($\delta^{57}Fe$ = –0.82 to –0.30‰, much lower than the predicted values of –0.15 to –0.04‰) were modified during subsolidus re-equilibration.

On the other hand, magnetite and ilmenite in the Middle and Upper Zones are mainly in contact with silicate minerals (Fig. 2f), which were last equilibrated with Fe-Ti oxides at ~950 °C (Pang et al. 2008b). Thus, redistributions of transition elements

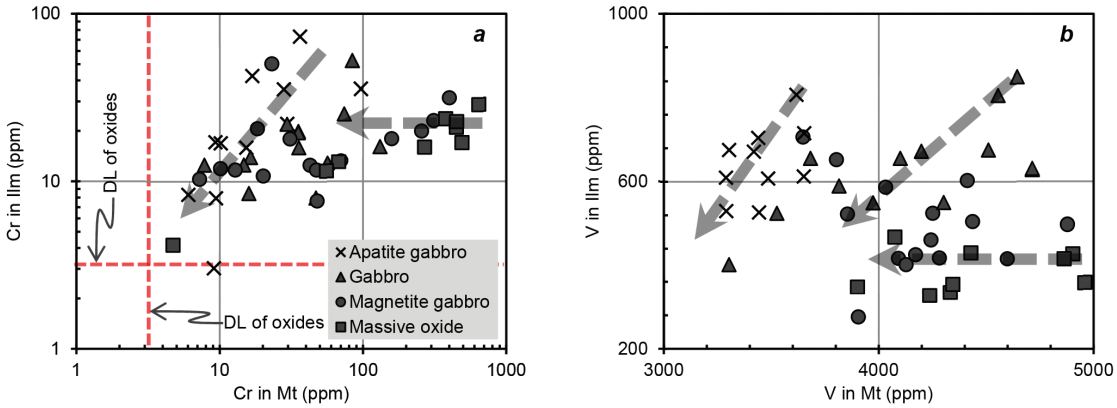

FIGURE 9. Binary plots for the average contents of (**a**) Cr in magnetite vs. Ni in ilmenite, and (**b**) V in magnetite vs. V in ilmenite for the different Panzhihua rock types. Abbreviations: Mt = Magnetite, Ilm = Ilmenite; DL = Detection Limit.

between magnetite and ilmenite in the Middle and Upper Zone rocks would not be significant upon cooling compared to those in the massive Fe-Ti oxide layers. Consequently, the transition elements display roughly positive correlations among magnetite, ilmenite, and clinopyroxene in the Middle and Upper Zone rocks with low proportions of Fe-Ti oxides (especially in the Upper Zone samples) (Figs. 8 and 9). Furthermore, ilmenite in contact with magnetite in the magnetite gabbro of the Lower Zone contains lower Cr and V than that in contact with silicates, giving additional support to the above interpretation (Table S3).

CONCLUSIONS AND IMPLICATIONS

Trace element variations among magnetite, ilmenite, and clinopyroxene from the Panzhihua layered intrusion are primarily controlled by magma compositions, co-crystallizing minerals, trapped liquid shift, and subsolidus re-equilibration. Prior removal of a sulfide liquid and the fractionation of chromite and/or Cr-magnetite at depth resulted in depletions of Ni, Co, and Cr in the parental magmas, and thus in the magnetite, ilmenite and clinopyroxene they produced. Fractional crystallization of olivine and clinopyroxene at deep levels also gave rise to the enrichment of incompatible trace elements in the parental magmas. In the Lower Zone, early co-crystallization of magnetite and clinopyroxene resulted in positive correlations in the transition metal contents (e.g., Ni, Cr, V, and Sc), while ilmenite crystallized somewhat after magnetite and clinopyroxene. In the Middle and Upper Zones, however, ilmenite crystallized concurrently with magnetite and clinopyroxene, which produced the negative Nb, Zr, Hf, and Ti anomalies in clinopyroxene. These results further support our proposed genetic model, in which the fractionation of silicates at depth and early Fe-Ti oxide saturation in the shallow magma chambers are key factors in the formation of the massive Fe-Ti oxide layers at Panzhihua (Zhang et al. 2011; Song et al. 2013; Zheng et al. 2014). The trapped intercumulus liquids may have significantly altered the original contents of incompatible trace elements (e.g., Zr, Nb, and Hf) in magnetite, ilmenite, and clinopyroxene and caused the distinct elemental heterogeneity of these elements in all the Lower Zone cumulus minerals; while such effects were insignificant in the Middle and Upper Zones. This interpretation is further supported by the finding that magnetite and clinopyroxene adjacent to hornblende rims have higher incompatible trace element contents than those not in contact with hornblende.

The reliability of using the elemental composition of any single cumulus mineral (e.g., clinopyroxene) and partition coefficients to back-calculate the parental magma composition of a layered intrusion is problematic, since the minerals may have been in competition for trace elements and/or experienced trapped liquid shift. Furthermore, we found that Fe-Ti oxides may have undergone extensive elemental re-equilibration by diffusion, which modified the original magmatic signature of the Lower Zone ilmenite. Thus, the critical processes controlling trace-element partitioning in cumulus minerals should be investigated before applying magnetite trace element geochemistry as a petrogenetic indicator to discriminate ore deposit types and their formation settings and mechanisms.

ACKNOWLEDGMENTS

This work was funded by CAS/SAFEA International Partnership Program for Creative Research Teams (Intraplate Mineralization Research Team; KZZD-EW-TZ-20), the strategic priority research program (B) of the Chinese Academy of Sciences (XDB18000000), the NSFC (41473024, 41373042, and 41473050), and the National Key R&D Program of China (2016YFC0600503). We acknowledge Sarah Dare and Dominique Tanner for their constructive and detailed reviews, and Fidel Costa for his suggestions and editorial handling. Special thanks are given to Dany Savard for providing the in-house standard magnetite BC-28 and geochemical calibration. Wen-Qin Zheng is appreciated for her effort in EPMA analysis. Fang-Zhen Teng, Aaron Brewer, and Cenozoic Geoscience Editing & Consultancy are thanked for polishing the language.

REFERENCES CITED

Aigner-torres, M., Blundy, J., Ulmer, P., and Pettke, T. (2007) Laser ablation ICPMS study of trace element partitioning between plagioclase and basaltic melts: an experimental approach. Contributions to Mineralogy and Petrology, 153, 647–667.

Ali, J.R., Thompson, G.M., Zhou, M.-F., and Song, X.-Y (2005) Emeishan large igneous province, SW China. Lithos, 79, 475–489.

Arndt, N., Jenner, G., Ohnenstetter, M., Deloule, E., and Wilson, A. (2005) Trace elements in the Merensky Reef and adjacent norites Bushveld Complex South Africa. Mineralium Deposita, 40, 550–575.

Bai, Z.-J., Zhong, H., Naldrett, A.J., Zhu, W.-G., and Xu, G.-W. (2012) Whole-rock and mineral composition constraints on the genesis of the Giant Hongge Fe–Ti–V oxide deposit in the Emeishan Large Igneous Province, Southwest China. Economic Geology, 107, 507–524.

Bai, Z.-J., Zhong, H., Li, C., Zhu, W.-G., He, D.-F., and Qi, L. (2014) Contrasting parental magma compositions for the Hongge and Panzhihua magmatic Fe–Ti–V oxide deposits, Emeishan large igneous province, SW China. Economic Geology, 109, 1763–1785.

Bai, Z.-J., Zhong, H., Li, C., Zhu, W.-G., He, D.-F., and Hu, W.-J. (2016) Association of cumulus apatite with compositionally unusual olivine and plagioclase in the Taihe Fe-Ti oxide ore-bearing layered mafic-ultramafic intrusion: Petrogenetic significance and implications for ore genesis. American Minerlogist, 101, 2168–2175.

Barnes, S. (1986) The effect of trapped liquid crystallization on cumulus mineral compositions in layered intrusions. Contributions to Mineralogy and Petrology, 93, 524–531.

Barnes, S.J., Maier, W.D., and Ashwal, L.D. (2004) Platinum-group element distribution in the main zone and upper zone of the Bushveld Complex, South Africa. Chemical Geology, 208, 293–317.

Beattie, P. (1994) Systematics and energetics of trace-element partitioning between olivine and silicate melts: Implications for the nature of mineral/melt partitioning. Chemical Geology, 117, 57–71.

Cawthorn, R.G. (1996) Layered Intrusions, 519 p. Elsevier Science.

—— (2007) Cr and Sr: Keys to parental magmas and processes in the Bushveld Complex, South Africa. Lithos, 95, 381–398.

—— (2013) Rare earth element abundances in apatite in the Bushveld Complex—A consequence of the trapped liquid shift effect. Geology, 41, 603–606.

Chen, L.-M., Song, X.-Y., Zhu, X.-K., Zhang, X.-Q., Yu, S.-Y., and Yi, J.-N. (2014) Iron isotope fractionation during crystallization and sub-solidus re-equilibration: Constraints from the Baima mafic layered intrusion, SW China. Chemical Geology, 380, 97–109.

Chung, S.L., and Jahn, B.M. (1995) Plume-lithosphere interaction in generation of the Emeishan flood basalts at the Permian-Triassic boundary. Geology, 23, 889–892.

Dare, S.A.S., Barnes, S.-J., and Beaudoin, G. (2012) Variation in trace element content of magnetite crystallized from a fractionating sulfide liquid, Sudbury, Canada: Implications for provenance discrimination. Geochimica et Cosmochimica Acta, 88, 27–50.

Dare, S.A.S., Barnes, S.-J., Beaudoin, G., Méric, J., Boutroy, E., and Potvin-Doucet, C. (2014) Trace elements in magnetite as petrogenetic indicators. Mineralium Deposita, 49, 785–796.

Dygert, N., Liang, Y., and Hess, P. (2013) The importance of melt TiO_2 in affecting major and trace element partitioning between Fe–Ti oxides and lunar picritic glass melts. Geochimica et Cosmochimica Acta, 106, 134–151.

Dygert, N., Liang, Y., Sun, C., and Hess, P. (2014) An experimental study of trace element partitioning between augite and Fe-rich basalts. Geochimica et Cosmochimica Acta, 132, 170–186.

Eales, H.V., and Cawthorn, R.G. (1996). The Bushveld Complex. In R.G. Cawthorn, Ed., Layered Intrusions, p. 181–229. Elsevier.

Egorova, V., and Latypov, R. (2013) Mafic–ultramafic sills: New insights from M- and S-shaped mineral and whole-rock compositional profiles. Journal of Petrology, 54, 2155–2191.

Fenner, C.N. (1929) The crystallization of basalts. American Journal of Science, 18, 225–253.

Forien, M., Tremblay, J., Barnes, S.-J., Burgisser, A., and Pagé, P. (2015) The role of viscous particle segregation in forming chromite layers from slumped crystal slurries: Insights from analogue experiments. Journal of Petrology, 56, 2425–2444.

Frost, B.R., and Lindsley, D.H. (1991) Occurrence of iron-titanium oxides in igneous rocks. Reviews in Mineralogy and Geochemistry, 25, 433–468.

Ganino, C., Arndt, N.T., Zhou, M.F., Gaillard, F., and Chauvel, C. (2008) Interaction of magma with sedimentary wall rock and magnetite ore genesis in the Panzhihua mafic intrusion, SW China. Mineralium Deposita, 43, 677–694.

Ghiorso, M.S. and Sack, R.O. (1995) Chemical mass transfer in magmatic processes. IV. A revised and internally consistent thermodynamic model for the interpolation and extrapolation of liquid-solid equilibria in magmatic systems at elevated temperatures and pressures. Contributions to Mineralogy and Petrology, 119, 197–212.

Godel, B., Barnes, S.-J., and Maier, W.D. (2011) Parental magma composition inferred from trace element in cumulus and intercumulus silicate minerals: An example from the Lower and Lower Critical Zones of the Bushveld Complex, South-Africa. Lithos, 125, 537–552.

Hart, S.R., and Dunn, T. (1993) Experimental cpx/melt partitioning of 24 trace elements. Contributions to Mineralogy and Petrology, 113, 1–8.

Hauri, E.H., Wagner, T.P., and Grove, T.L. (1994) Experimental and natural partitioning of Th, U, Pb and other trace elements between garnet, clinopyroxene and basaltic melts. Chemical Geology, 117, 149–166.

Hou, T., Zhang, Z., Encarnacion, J., Santosh, M., and Sun, Y. (2013) The role of recycled oceanic crust in magmatism and metallogeny: Os–Sr–Nd isotopes, U–Pb geochronology and geochemistry of picritic dykes in the Panzhihua giant Fe–Ti oxide deposit, central Emeishan large igneous province, SW China. Contributions to Mineralogy and Petrology, 165, 805–822.

Howarth, G.H., and Prevec, S.A. (2013) Trace element, PGE, and Sr–Nd isotope geochemistry of the Panzhihua mafic layered intrusion, SW China: Constraints on ore-forming processes and evolution of parent magma at depth in a plumbing-system. Geochimica et Cosmochimica Acta, 120, 459–478.

Howarth, G.H., Prevec, S.A., and Zhou, M.-F. (2013) Timing of Ti-magnetite crystallisation and silicate disequilibrium in the Panzhihua mafic layered intrusion: Implications for ore-forming processes. Lithos, 170–171, 73–89.

Jakobsen, J.K., Tegner, C., Brooks, C.K., Kent, A.J.R., Lesher, C.E., Nielsen, T.F.D., and Wiedenbeck, M. (2010) Parental magma of the Skaergaard intrusion: constraints from melt inclusions in primitive troctolite blocks and FG-1 dykes. Contributions to Mineralogy and Petrology, 159, 61–79.

Jang, Y.D., and Naslund, H.R. (2001) Major and trace element composition of Skaergaard plagioclase; geochemical evidence for changes in magma dynamics during the final stage of crystallization of the Skaergaard intrusion. Contributions to Mineralogy and Petrology, 140, 441–457.

—— (2003) Major and trace element variation in ilmenite in the Skaergaard Intrusion: petrologic implications. Chemical Geology, 193, 109–125.

Jourdan, F., Bertrand, H., Scharer, U., Blichert-Toft, J., Feraud, G., and Kampunzu, A.B. (2007) Major and trace element and Sr, Nd, Hf and Pb isotope compositions of the Karoo large igneous province, Botswana-Zimbabwe: Lithosphere vs mantle plume contribution. Journal of Petrology, 48, 1043–1077.

Kamenetsky, V.S., Chung, S.L., Kamenetsky, M.B., and Kuzmin, D.V. (2012) Picrites from the Emeishan Large Igneous Province, SW China: A compositional continuum in primitive magmas and their respective mantle sources. Journal of Petrology, 53, 2095–2113.

Kloeck, W., and Palme, H. (1988) Partitioning of siderophile and chalcophile elements between sulfide, olivine, and glass in a naturally reduced basalt from Disko Island, Greenland. In G. Ryder, Ed., Proceedings of the Lunar and Planetary Science Conference, 18, 471–483. Pergamon, New York.

Laubier, M., Grove, T.L., and Langmuir, C.H. (2014) Trace element mineral/melt partitioning for basaltic and basaltic andesitic melts: An experimental and laser ICP-MS study with application to the oxidation state of mantle source regions. Earth and Planetary Science Letters, 392, 265–278.

Liu, Y., Hu, Z., Gao, S., Günther, D., Xu, J., Gao, C., and Chen, H. (2008) In situ analysis of major and trace elements of anhydrous minerals by LA-ICP-MS without applying an internal standard. Chemical Geology, 257, 34–43.

Liu, P.-P., Zhou, M.-F., Chen, W.T., Boone, M., and Cnudde, V. (2014) Using multiphase solid inclusions to constrain the origin of the Baima Fe–Ti–(V) oxide deposit, SW China. Journal of Petrology, 55, 951–976.

Liu, P.-P., Zhou, M.-F., Chen, W.T., Gao, J.-F., and Huang, X.-W. (2015) In-situ LA-ICP-MS trace elemental analyses of magnetite: Fe–Ti–(V) oxide-bearing mafic–ultramafic layered intrusions of the Emeishan Large Igneous Province, SW China. Ore Geology Reviews, 65, 853–871.

Luan, Y., Song, X.-Y., Chen, L.-M., Zheng, W.-Q., Zhang, X.-Q., Yu, S.-Y., She, Y.-W., Tian, X.-L., and Ran, Q.-Y. (2014) Key factors controlling the accumulation of the Fe–Ti oxides in the Hongge layered intrusion in the Emeishan large igneous province, SW China. Ore Geology Reviews, 57, 518–538.

Lundgaard, K.L., Tegner, C., Cawthorn, R.G., Kruger, F.J., and Wilson, J.R. (2006) Trapped intercumulus liquid in the Main Zone of the eastern Bushveld Complex, South Africa. Contributions to Mineralogy and Petrology, 151, 352–369.

Maier, W.D., Barnes, S.J., and Groves, D.I. (2013) The Bushveld Complex, South Africa: formation of platinum–palladium, chrome- and vanadium-rich layers via hydrodynamic sorting of a mobilized cumulate slurry in a large, relatively slowly cooling, subsiding magma chamber. Miner Deposita, 48, 1–56.

Namur, O., Charlier, B., Toplis, M.J., Higgins, M.D., Liegeois, J.P., and Vander Auwera, J. (2010) Crystallization sequence and magma chamber processes in the ferrobasaltic Sept Iles layered intrusion, Canada. Journal of Petrology, 51, 1203–1236.

Nielsen, T.F.D. (2004) The shape and volume of the Skaergaard intrusion, Greenland: Implications for mass balance and bulk composition. Journal of Petrology, 45(3), 507–530.

Pang, K.N., Li, C.S., Zhou, M.F., and Ripley, E.M. (2008a) Abundant Fe–Ti oxide inclusions in olivine from the Panzhihua and Hongge layered intrusions, SW China: evidence for early saturation of Fe–Ti oxides in ferrobasaltic magma. Contributions to Mineralogy and Petrology, 156, 307–321.

Pang, K.N., Zhou, M.F., Lindsley, D., Zhao, D., and Malpas, J. (2008b) Origin of Fe–Ti oxide ores in mafic intrusions: Evidence from the Panzhihua intrusion, SW China. Journal of Petrology, 49, 295–313.

Pang, K.N., Li, C.S., Zhou, M.F., and Ripley, E.M. (2009) Mineral compositional constraints on petrogenesis and oxide ore genesis of the late Permian Panzhihua layered gabbroic intrusion, SW China. Lithos, 110, 199–214.

Panxi Geological Unit (1984) Mineralization and exploration forecasting of V–Ti magnetite deposits in the Panzhihua–Xichang region. Unpublished, Panxi Geological Unit (in Chinese).

Peach, C.L., Mathez, E.A., and Keays, R.R. (1990) Sulfide melt-silicate melt distribution coefficients for noble metals and other chalcophile elements as deduced from MORB: Implications for partial melting. Geochimica et Cosmochimica Acta, 54, 3379–3389.

Pedersen, A.K. (1979) Basaltic glass with high-temperature equilibrated immiscible sulfide bodies with native iron from Disko, central west Greenland. Contributions to Mineralogy and Petrology, 69, 397–407.

Rajamani, V., and Naldrett, A.J. (1978) Partitioning of Fe, Co, Ni, and Cu between sulfide liquid and basaltic melts and the composition of Ni–Cu sulfide deposits. Economic Geology, 73, 82–93.

She, Y.-W., Yu, S.-Y., Song, X.-Y., Chen, L.-M., Zheng, W.-Q., and Luan, Y. (2014) The formation of P-rich Fe–Ti oxide ore layers in the Taihe layered intrusion, SW China: Implications for magma-plumbing system process. Ore Geology

Reviews, 57, 539–559.
She, Y.-W., Song, X.-Y., Yu, S.-Y., and He, H.-L. (2015) Variations of trace element concentration of magnetite and ilmenite from the Taihe layered intrusion, Emeishan large igneous province, SW China: Implications for magmatic fractionation and origin of Fe–Ti–V oxide ore deposits. Journal of Asian Earth Sciences, 113, 1117–1131.
Shellnutt, J.G., Denyszyn, S.W., and Mundil, R. (2012) Precise age determination of mafic and felsic intrusive rocks from the Permian Emeishan large igneous province (SW China). Gondwana Research, 22, 118–126.
Song, X.Y., Zhou, M.F., Hou, Z.Q., Cao, Z.M., Wang, Y.L., and Li, Y.G. (2001) Geochemical constraints on the mantle source of the upper permian Emeishan continental flood basalts, southwestern China. International Geology Review, 43, 213–225.
Song, X.Y., Zhou, M.F., Cao, Z.M., and Robinson, P.T. (2004) Late permian rifting of the South China Craton caused by the Emeishan mantle plume? Journal of the Geological Society, 161, 773–781.
Song, X.Y., Qi, H.W., Robinson, P.T., Zhou, M.F., Cao, Z.M., and Chen, L.M. (2008) Melting of the subcontinental lithospheric mantle by the Emeishan mantle plume; evidence from the basal alkaline basalts in Dongchuan, Yunnan, Southwestern China. Lithos, 100, 93–111.
Song, X.Y., Qi, H.W., Hu, R.Z., Chen, L.M., Yu, S.Y., and Zhang, J.F. (2013) Formation of thick stratiform Fe–Ti oxide layers in layered intrusion and frequent replenishment of fractionated mafic magma: Evidence from the Panzhihua intrusion, SW China. Geochemistry, Geophysics, Geosystems, 14, 712–732.
Tanner, D., Mavrogenes, J.A., Arculus, R.J., and Jenner, F.E. (2014) Trace element stratigraphy of the Bellevue Core, Northern Bushveld: Multiple magma injections obscured by diffusive processes. Journal of Petrology, 55, 859–882.
Tegner, C., Cawthorn, R.G., and Kruger, F.J. (2006) Cyclicity in the main and upper zones of the Bushveld complex, South Africa: Crystallization from a zoned magma sheet. Journal of Petrology, 47(11), 2257–2279.
Thy, P., Lesher, C.E., Nielsen, T.F.D., Brooks, C.K. (2006) Experimental constraints on the Skaergaard liquid line of descent. Lithos, 92, 154–180.
Toplis, M.J., and Carroll, M.R. (1995) An experimental study of the influence of oxygen fugacity on Fe–Ti oxide stability, phase relations, and mineral-melt equilibria in ferro-basaltic systems. Journal of Petrology, 36, 1137–1170.
Tribuzio, R., Tiepolo, M., Vannucci, R., and Bottazzi, P. (1999) Trace element distribution within olivine-bearing gabbros from the Northern Apennine ophiolites (Italy): Evidence for post-cumulus crystallization in MOR-type gabbroic rocks. Contributions to Mineralogy and Petrology, 134, 123–133.
van Kan Parker, M., Mason, P.R.D., and van Westrenen, W. (2011) Trace element partitioning between ilmenite, armalcolite and anhydrous silicate melt: Implications for the formation of lunar high-Ti mare basalts. Geochimica et Cosmochimica Acta, 75, 4179–4193.
Vantongeren, J.A., and Mathez, E.A. (2013) Incoming magma composition and style of recharge below the Pyroxenite Marker, Eastern Bushveld Complex, South Africa. Journal of Petrology, 54, 1585–1605.
Wager, L.R., and Brown, G.M. (1967) Layered Igneous Rocks. Oliver and Boyd, Edinburgh.
Xing, C.M., Wang, C.Y., and Li, C.Y. (2014) Trace element compositions of apatite from the middle zone of the Panzhihua layered intrusion, SW China: Insights into the differentiation of a P- and Si-rich melt. Lithos, 204, 188–202.
Xu, Y.G., Chung, S.L., Jahn, B.M., and Wu, G.Y. (2001) Petrologic and geochemical constraints on the petrogenesis of Permian-Triassic Emeishan flood basalts in southwestern China. Lithos, 58, 145–168.
Xu, Y.G., He, B., Chung, S.L., Menzies, M.A., and Frey, F.A. (2004) Geologic, geochemical, and geophysical consequences of plume involvement in the Emeishan flood-basalt province. Geology, 32, 917–920.
Zhang, Y.-X., Luo, Y.-N., and Yang, C.-X. (1988) The Panxi Rift. Geological Press, Beijing (in Chinese).
Zhang, Z.C., Mahoney, J.J., Mao, J.W., and Wang, F.H. (2006) Geochemistry of picritic and associated basalt flows of the western Emeishan flood basalt province, China. Journal of Petrology, 47, 1997–2019.
Zhang, Z.C., Li, Y., Zhao, L., and Ai, Y. (2007) Geochemistry of three layered mafic-ultramafic intrusions in the Panxi area and constraints on their sources. Acta Petrologica Sinica, 23, 2339–2352.
Zhang, X.-Q., Zhang, J.-F., Yuan, P., Song, X.-Y., Guan, J.-X., and Deng, Y.-F. (2011) Implications of compositions of plagioclase and olivine on the formation of the Panzhihua V–Ti magnetite deposit, Sichuan Province. Acta Petrologica Sinica, 27, 3675–3688 (in Chinese with English abstract).
Zhang, X.-Q., Song, X.-Y., Chen, L.-M., Xie, W., Yu, S.-Y., Zheng, W.-Q., Deng, Y.-F., Zhang, J.-F., and Gui, S.-G. (2012) Fractional crystallization and the formation of thick Fe–Ti–V oxide layers in the Baima layered intrusion, SW China. Ore Geology Reviews, 49, 96–108.
Zheng, W.-Q., Deng, Y.-F., Song, X.-Y., Chen, L.-M., Yu, S.-Y., Zhou, G.-F., Liu, S.-R., and Xiang, J.-X. (2014) Composition and genetic significance of the ilmenite of the Panzhihua intrusion. Acta Petrologica Sinica, 30, 1432–1442.
Zhong, H., and Zhu, W.-G. (2006) Geochronology of layered mafic intrusions from the Pan–Xi area in the Emeishan large igneous province, SW China. Mineralium Deposita, 41, 599–606.
Zhong, H., Zhou, X.H., Zhou, M.F., Sun, M., and Liu, B.G. (2002) Platinum-group element geochemistry of the Hongge Fe-V-Ti deposit in the Pan-Xi area, southwestern China. Mineralium Deposita, 37(2), 226–239.
Zhong, H., Qi, L., Hu, R.-Z., Zhou, M.-F., Gou, T.-Z., Zhu, W.-G., Liu, B.-G., and Chu, Z.-Y. (2011) Rhenium-osmium isotope and platinum-group elements in the Xinjie layered intrusion, SW China: Implications for source mantle composition, mantle evolution, PGE fractionation and mineralization. Geochimica et Cosmochimica Acta, 75, 1621–1641.
Zhou, M.-F., Yan, D.-P., Kennedy, A.K., Li, Y., and Ding, J. (2002) SHRIMP U–Pb zircon geochronological and geochemical evidence for Neoproterozoic arc-magmatism along the western margin of the Yangtze Block, South China. Earth and Planetary Science Letters, 196, 51–67.
Zhou, M.F., Robinson, P.T., Lesher, C.M., Keays, R.R., Zhang, C.J., and Malpas, J. (2005) Geochemistry, petrogenesis and metallogenesis of the Panzhihua gabbroic layered intrusion and associated Fe–Ti–V oxide deposits, Sichuan Province, SW China. Journal of Petrology, 46, 2253–2280.
Zhou, M.F., Arndt, N.T., Malpas, J., Wang, C.Y., and Kennedy, A.K. (2008) Two magma series and associated ore deposit types in the Permian Emeishan large igneous province, SW China. Lithos, 103, 352–368.
Zhou, M.-F., Chen, W.T., Wang, C.Y., Prevec, S.A., Liu, Patricia P., and Howarth, G.H. (2013) Two stages of immiscible liquid separation in the formation of Panzhihua-type Fe-Ti-V oxide deposits, SW China. Geoscience Frontiers, 4(5), 481–502.

Manuscript received April 10, 2016
Manuscript accepted December 23, 2016
Manuscript handled by Fidel Costa